Proceedings of the 30th International Cosmic Ray Conference
Rogelio Caballero, Juan Carlos D'Olivo, Gustavo Medina-Tanco,
Lukas Nellen, Federico A. Sánchez, José F. Valdés-Galicia (eds.)
Universidad Nacional Autónoma de México,
Mexico City, Mexico, 2008

Vol. 2 (OG part 1), pages 803–806

30TH INTERNATIONAL COSMIC RAY CONFERENCE

Crab nebula spectrum as seen by H.E.S.S.

B. KHÉLIFI[1], C. MASTERSON[2], S. PITA[3], E. OÑA-WILHELMI[3] FOR THE H.E.S.S. COLLABORATION
[1]*Laboratoire Leprince-Ringuet, Ecole Polytechnique/IN2P3/CNRS, Palaiseau, France*
[2]*Dublin Institute for Advanced Studies, 5 Merrion Square, Dublin 2, Ireland*
[3]*AstroParticule et Cosmologie, Paris VII/IN2P3/CNRS, Paris, France*
khelifi@llr.in2p3.fr

Abstract: The H.E.S.S. stereoscopic Cherenkov telescope system has observed the Crab nebula since December 2003 with the complete four-telescope array. The stable signal from this pulsar wind nebula (PWN) has been used to verify the performance and calibration of the instrument thanks to its high flux compared to the H.E.S.S sensitivity. These observations allow us also to study the radiation mechanisms of this PWN, in particular by focusing on the high energy part of its energy spectrum, where gamma-ray emission at energies above 30 TeV has been detected.

Introduction

The Crab nebula was discovered at very high energies (VHE; >100 GeV) in 1989 [1] and the emission has been confirmed by a number of other experiments (e.g. [2, 3, 4]). This pulsar wind nebula (PWN) has a high flux relative to other known VHE sources and its emission is expected to be stable. As a result, the Crab nebula is commonly used as a standard 'calibration candle' for the ground-based gamma-ray detectors, and a particular attention is paid here to the control of the analysis chain accuracy. Indeed, the detector ageing results from a decrease of the overall optical efficiency (a combination of mirrors, light-cones, and photomultipliers degradation) and from ageing of electronics components of cameras. The detector response is measured, calibrated [5] and used for the data analysis [6].

Important questions on the origin of the non-thermal emission of the Crab nebula remain. It is commonly admitted that its spectral energy distribution (SED) can be well-reproduced with a mechanism based on a synchrotron self-Compton (SSC) emission of high energy electrons/positrons (e.g. [7]) even if a contribution from proton radiation is not excluded at high energies (e.g. [8]). However, the acceleration mechanisms of these leptons and hadrons are still under investigation (Cf. [9] for a recent review). Thus, multi-wavelength observations are still necessary to understand the underlying physics, in particular observations of VHE gamma-rays above 30 TeV.

H.E.S.S. observations and data analysis

The Crab nebula has been observed with the complete array for 58.4 hours from December 2003 to December 2006. After data-quality selection based on good weather conditions and good detector operation, an exposure of 29.4 hours live-time is obtained. The periods of the Crab observations suffer sometimes of poor weather conditions in Namibia. All observations were taken in *wobble* mode whereby the source is alternately offset by a fixed distance within the field of view, alternating between 28 minutes runs in positive and negative declination (or right ascension) directions.

In table 1 we present, for each observation period considered, the live-time (in hours), mean zenith angle (in degrees), mean position (in degrees) of the Crab pulsar position relative to the centre of the field of view and mean optical efficiency (in percent) of the detection system.

The data are processed with the HAP (H.E.S.S. Analysis Package) software as follows. In order

Year	2004	2005	2006	All
Live-time [h]	20.6	5.4	3.4	29.4
Zenith Angle [deg]	52.2	47.7	49.2	51.1
Offset [deg]	0.65	0.58	0.70	0.65
OptEff [%]	8.3	7.8	7.0	8.1

Table 1: Summary of the Crab observations. The row descriptions are given in the text.

to reject the overwhelming background of night-sky diffuse light and hadronic showers, a two-level image cleaning is performed to remove pixels containing only background noise. After image cleaning, the Hillas parameters [10] are computed. For comparison, two methods are used to reconstruct the characteristics of the atmospheric showers, i.e. the impact parameter (D), the shower maximum (H) and the shower direction. The first method [6], called hereafter *Hillas*, is based on a geometrical reconstruction of the shower characteristics from the Hillas parameters (tracks of the projected direction of the shower in the field of view). The second one, called *Model3D* [11], uses a model of the atmospheric shower as a 'Cherenkov ellipsoid' and its parameters are adjusted to the camera images. Cuts are applied to the parameters derived by these methods to improve the signal to (hadronic) noise ratio. For the *Model3D* analysis, the standard cuts of the *Hillas* analysis are applied together with cuts on the 'Cherenkov ellipsoid' size. The remaining background is estimated from regions at same distance from the field of view centre as the Crab pulsar position for the observations (cf. fig. 9 of [6]).

The energy of each event is estimated from D, H and the images charges within the Hillas ellipses (Q). Look-up tables given the image charges as a function of energy (E), D and H ($Q = f(E, D, H)$ are derived from gamma-ray simulations made with Kaskade [12] for different fixed energies, zenith angles, offsets and optical efficiencies. Given the measured Q, D and H, inverting the tables provides an estimation of the event energy. To determine the energy spectrum, the instrument response functions (effective areas and energy resolutions) are derived from the same gamma-ray simulations, and a forward-folding algorithm developed by the CAT collaboration [13] is used. A likelihood fit is used to adjust different spectral shape hypotheses. A test of the hypotheses with a likelihood ratio is made to determine the spectrum shape that best adjusts to the data.

H.E.S.S. results

The main results of the analysis of the Crab observations are given in table 2. For each method of shower reconstruction and for each year, the number of gamma-rays above the analysis energy threshold, the significance and the integral flux above 1 TeV are listed. A strong signal is detected and, independently of the year and the analysis method, the integral flux is basically constant, illustrating the good correction for the effects of the detector ageing.

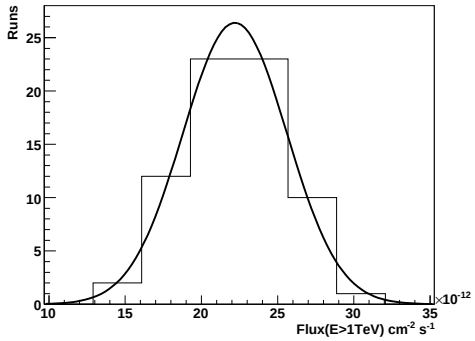

Figure 1: Distribution of the run-wise integral fluxes above 1 TeV for the *Hillas* analysis.

The run-wise fluxes are also computed and their distribution is given in fig. 1 for the *Hillas* analysis. It follows a Gaussian distribution (black line) with a χ^2/dof of $0.50/3$. The best-fit parameters are Mean $= 2.22 \pm 0.04$ and Sigma $= 0.34 \pm 0.02$ in units of $10^{-11}\text{cm}^{-2}\text{s}^{-1}$. The flux derived is thus compatible with a steady flux with Gaussian fluctuations of $\sim 15\%$.

	Hillas	*Model3D*
Φ_0^{PL}	3.52 ± 0.04	3.46 ± 0.04
Γ^{PL}	2.60 ± 0.01	2.61 ± 0.01
Φ_0^{EC}	3.53 ± 0.04	3.48 ± 0.04
Γ^{EC}	2.40 ± 0.03	2.42 ± 0.03
E_c^{EC}	16.7 ± 2.5	16.1 ± 2.5
λ^{EC}	74.4	66.6

Table 3: Summary of spectrum fits. The row descriptions are given in the text.

For both analyses, the energy spectrum is computed for two different spectral hypotheses: a pure power-law $\mathscr{H}_0$ ($\text{d}N/\text{d}E_{\text{PL}} = \Phi_0 \times E^{-\Gamma}$)

Method	Year	Excess [γ]	Significance [σ]	$F_{>1\,\mathrm{TeV}}$ [$\times 10^{-11}\mathrm{cm}^{-2}\mathrm{s}^{-1}$]
Hillas	2004	5788	122	2.22 ± 0.07
	2005	1674	70	2.18 ± 0.06
	2006	1069	57	2.41 ± 0.10
	All	8531	151	2.22 ± 0.04
Model3D	2004	5208	130	2.20 ± 0.06
	2005	1612	74	2.13 ± 0.18
	2006	1008	59	2.37 ± 0.12
	All	7828	161	2.22 ± 0.05

Table 2: Results of the observations. The column descriptions are given in the text.

and a power-law with an exponential cut-off $\mathscr{H}_1$ ($\mathrm{d}N/\mathrm{d}E_{\mathrm{EC}} = \Phi_0 \times E^{-\Gamma} \times \mathrm{e}^{-E/E_c}$). The fit results are listed in table 3. The parameter Φ_0 is in units of $10^{-11}\mathrm{cm}^{-2}\mathrm{s}^{-1}\mathrm{TeV}^{-1}$, E_c in TeV. λ is the ratio between the maximum likelihood of the $\mathscr{H}_1$ fit over the $\mathscr{H}_0$ fit and its distribution follows asymptotically a χ^2 law with one degree of freedom. From this parameter and independently of the analysis method used, it can clearly be seen that the fitted spectrum shape is not compatible with a pure power-law with a probability less than 10^{-6}. The use of a 'parabolic' spectrum shape ($E^{-\alpha-\beta\log(E)}$) fits the data equally well as a power-law with an exponential cut-off. Note that the fit results are compatible between the different analyses.

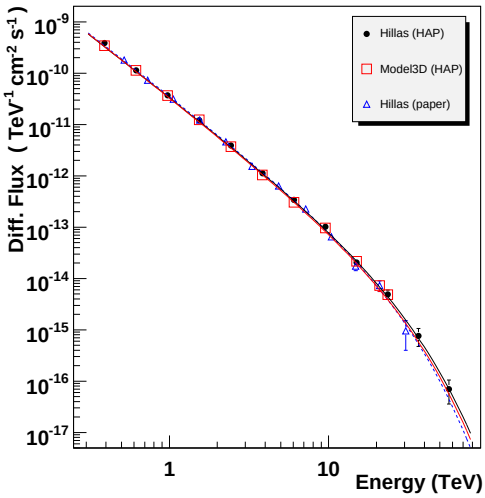

Figure 2: Comparison of the Crab spectrum fits between this analysis and that published in [6]. The lines are the best-fit shapes.

Figure 2 shows the Crab spectrum derived with these two analyses carried out with the HAP software, together with the H.E.S.S. spectrum published in [6]. In the following, the results of the $\mathscr{H}_1$ fit for the *Hillas* analysis are used and the flux measurements for each energy bin (differential flux) are given in table 4. Here, the measurements on high energy bins above 30 TeV should be emphasised in which a signal is detected at the level of $\sim 6\sigma$. A signal is detected significantly at the highest energies which allows the spectrum curvature to be measured more accurately . Figure 3 shows the comparison of the best-fit parameters Γ and $1/E_c$ between these analyses and the results from [6]. The parameters are quite compatible between these and the exponential cut-off energy, E_c, is compatible with $\sim$15 TeV.

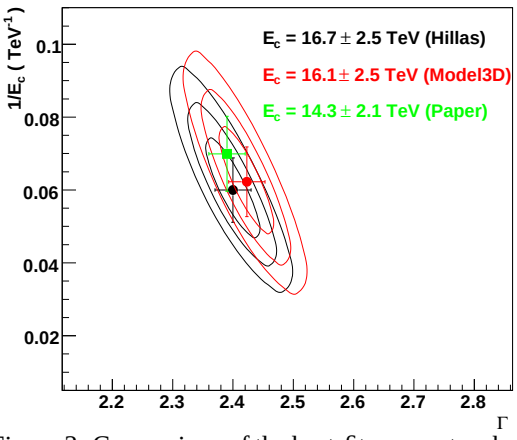

Figure 3: Comparison of the best-fit parameters between this analysis and those published in [6].

Conclusions

Analysis of Crab data carried out with the new software framework HAP yields results which are consistent with those published previously by H.E.S.S. in [6]. The measured Crab flux is compatible with

Mean Energy	Significance $[\sigma]$	$\frac{\mathrm{d}N}{\mathrm{d}E}$ $[\mathrm{cm}^{-2}\mathrm{s}^{-1}\mathrm{TeV}^{-1}]$
0.39	16.7	$(3.87 \pm 0.38) \times 10^{-10}$
0.62	73.4	$(1.14 \pm 0.03) \times 10^{-10}$
0.97	78.4	$(3.72 \pm 0.08) \times 10^{-11}$
1.54	67.7	$(1.21 \pm 0.03) \times 10^{-11}$
2.43	55.9	$(3.93 \pm 0.12) \times 10^{-12}$
3.84	41.3	$(1.13 \pm 0.05) \times 10^{-12}$
6.06	30.2	$(3.40 \pm 0.19) \times 10^{-13}$
9.54	22.4	$(1.01 \pm 0.07) \times 10^{-13}$
15.0	12.4	$(2.05 \pm 0.27) \times 10^{-14}$
23.5	7.9	$(4.91 \pm 1.00) \times 10^{-15}$
36.7	4.1	$(7.56 \pm 2.84) \times 10^{-16}$
57.0	3.8	$(7.22 \pm 3.40) \times 10^{-17}$

Table 4: Flux measurements for each energy bin for the *Hillas* analysis.

a steady flux between December 2003 and December 2006, indicating that all effects of the detector ageing are correctly taken into account. The integral flux above 1 TeV is $F(> 1\,\mathrm{TeV}) = (2.22 \pm 0.07) \times 10^{-11}\,\mathrm{cm}^{-2}\mathrm{s}^{-1}$. Its energy spectrum is not compatible with a pure power-law shape and is well-represented by a power-law with an exponential cut-off ($E_c = 16.7 \pm 2.5\,\mathrm{TeV}$).

Comparing the results of different analyses presented here, one finds that the differences of flux and spectrum index estimated are well within the systematics detailed in [6].

A clear signal is detected above 30 TeV which allows the curved nature of the Crab nebula spectrum to be clearly confirmed. This measured spectrum seems to be still compatible with a SSC scenario in the Klein-Nishina regime as described in [7]. An adjustment of the fit parameters of this radiation model on our data is still necessary to confirm this scenario.

Acknowledgements

The support of the Namibian authorities and of the University of Namibia in facilitating the construction and operation of H.E.S.S. is gratefully acknowledged, as is the support by the German Ministry for Education and Research (BMBF), the Max Planck Society, the French Ministry for Research, the CNRS-IN2P3 and the Astroparticle Interdisciplinary Programme of the CNRS, the U.K. Science and Technology Facilities Council (STFC), the IPNP of the Charles University, the Polish Ministry of Science and Higher Education, the South African Department of Science and Technology and National Research Foundation, and by the University of Namibia. We appreciate the excellent work of the technical support staff in Berlin, Durham, Hamburg, Heidelberg, Palaiseau, Paris, Saclay, and in Namibia in the construction and operation of the equipment.

References

[1] Weekes T.C. *et al.*, 1989, ApJ 342, 379
[2] Aharonian F.A. *et al.* (HEGRA coll.), 2000, ApJ 539, 317
[3] Masterson C. *et al.*, 2001, High Energy Gamma-Ray Astronomy, AIP 558, 753
[4] Albert J. *et al.* (MAGIC coll.), 2007, astro-ph/07053244
[5] Aharonian F.A. *et al.* (H.E.S.S. coll.), 2004, APh 22, 119
[6] Aharonian F.A. *et al.* (H.E.S.S. coll.), 2006, A&A 457, 899
[7] Horns D. and Aharonian F.A., 2004, ESASP 552, 439
[8] Amato E., Guetta D. and Blasi P., 2003, A&A 402, 827
[9] Kirk J.G., Lyubarsky Y. and Pétri J., 2007, astro-ph/0703116v2
[10] Hillas A., 1985, Proc. 19nd I.C.R.C., Vol. 3, 445
[11] Lemoine M. *et al.*, 2006, APh 25, 195
[12] Kertzman M. P. and Sembroski G. H., 1994, NIM A 343, 629
[13] Piron F. *et al.*, 2001, A&A 374, 895